Evolution of collectivity in neutron-rich nuclei in the ^{132}Sn region

Ritesh Kshetri and M. Saha Sarkar
Saha Institute of Nuclear Physics, 1/AF Bidhan Nagar, Calcutta 700064, India

S. Sarkar*
Department of Physics, The University of Burdwan, Golapbag, Burdwan 713104, India
(Received 1 June 2006; published 13 September 2006)

Motivated by the observed regularity in the energy spectra and the structure of the shell model wave functions for the levels of ^{137}Te and ^{137}I, a few weakly and moderately deformed neutron-rich odd-A nuclei above the doubly magic nucleus ^{132}Sn were studied using the particle rotor model (PRM). The calculated energy spectra and branching ratios agree reasonably well with the most recent experimental data. In a few cases ambiguity in level ordering was resolved and spin-parities were assigned to the levels. Observed octupole correlation in some of these nuclei is discussed in the light of the present results.

DOI: 10.1103/PhysRevC.74.034314 PACS number(s): 21.60.Ev, 27.60.+j, 21.10.Re, 21.60.Cs

I. INTRODUCTION

Neutron-rich nuclei above the doubly closed ^{132}Sn core are of current interest both experimentally and theoretically. It is interesting to note that after ^{16}O, ^{132}Sn ($N/Z = 1.64$) exhibits the strongest shell closure and lies near the neutron-drip line, eight neutrons away from the naturally abundant heaviest isotope of Sn (^{124}Sn) on the line of stability. Fission fragment γ-spectroscopic studies with large detector arrays reveal many intriguing aspects of nuclear structure for this very neutron-rich close-to-drip line mass region. Recent experimental studies of a number of Sn, Sb, Te, I, Xe, Cs, and Ba isotopes with $N = 82$–87 furnish information for phenomenological and systematic understanding of nuclear structure for this mass region. They also provide a basis for studying empirical N-N interaction in this exotic n-rich environment as well as a testing ground for shell model and other phenomenological nuclear models. These nuclei with $50 \leqslant Z \leqslant 56$ and $82 \leqslant N \leqslant 87$ lie on or close to the astrophysical r-process path and are connected by β decays. Many of these extremely n-rich nuclei are still not accessible for spectroscopic studies. Thus reliance on the theoretical models is inescapable. It is therefore of interest to apply and check the validity and improve upon the theoretical models in the light of the available data for this region. This may be helpful for providing a guidance for experimental studies of spectroscopic properties of nuclei in the region not yet investigated.

Shell model calculations for nuclei with a few valence particles in the $\pi\,[1g_{7/2}, 2d_{5/2}, 2d_{3/2}, 3s_{1/2}, 1h_{11/2}]$ and $\nu\,[1h_{9/2}, 2f_{7/2}, 2f_{5/2}, 3p_{3/2}, 3p_{1/2}, 1i_{13/2}]$ orbitals above the ^{132}Sn core gave excellent results [1–3] for the energy levels and other spectroscopic properties. It has been shown in Ref. [2] that with increasing nucleon number the shell model wave functions show tremendous configuration mixing even for the yrast states in ^{137}Te and ^{137}I. This indicated an onset of mild collectivity in these nuclei. This fact is also supported by the gradual change of $R_4 = (E_{4^+}/E_{2^+})$ values of the even-even Te isotopes from 1.23 (^{134}Te) to 2.04 (^{138}Te) [4] showing evolution toward collectivity. Similarly, the relative values of quadrupole deformation, $\beta_2/\beta_2(\textit{single particle})$, for even-even $^{138-146}$Ba are found to be 3.28(6), 4.4(10), 5.62(15), 6.82(20), and 7.68(14), respectively [5], indicating again gradual onset of collectivity with increasing neutron number. There are also theoretical suggestions and experimental hints [6] that beyond the ^{132}Sn core nuclear deformation shows up around $N = 87$ and appearance of deformation for nuclei on or near the r-process path may significantly influence the r-process flow [6]. It thus seems interesting and important to study the evolution of collectivity in these n-rich weakly/moderately deformed nuclei. Another motivation of the present study is that the odd-A nuclei with $N = 85$ lie in a region of transition, at the border of the predicted quadrupole-octupole correlation island. Pronounced octupole correlation was claimed to be observed in ^{139}Xe and ^{141}Ba [7]. But later Urban *et al.* [8] contradicted it, suggesting coupling of octupole-quadrupole vibrations as the probable mode of excitation. So the theoretical investigations into the structure of these nuclei offer an added opportunity to decide on the probable excitation mechanism.

For a large number of valence nucleons ($\geqslant$6), the shell model calculations in the previously mentioned valence space become computationally difficult because of the very large dimensionality of the matrices involved. Moreover, even this set of basis states used may be insufficient with the increase in collectivity. So we have studied the structure of a few of these weakly to moderately deformed neutron-rich nuclei having new experimental information, using a version of the particle rotor model (PRM) [9]. The advantage of this version is that the experimental energies of the core can be directly fed in as input. The model can be applied to very weakly deformed systems with collective nonrotational (vibrational, say) cores and also to strongly deformed systems with rotational cores [10].

In this work, a few odd-A nuclei with $N = 84$–87, namely, $^{137}_{53}I_{84}$, $^{139}_{55}Cs_{84}$, $^{137}_{52}Te_{85}$, $^{139}_{54}Xe_{85}$, $^{141}_{56}Ba_{85}$, $^{139}_{53}I_{86}$, $^{139}_{52}Te_{87}$, and $^{141}_{54}Xe_{87}$ have been studied. The theoretical results have reproduced the experimental spectra satisfactorily in most of

*Present address: Department of Physics, Bengal Engineering and Science University, Shibpur, Howrah-711103, India.

the cases showing the success of this model. In many of these nuclei, the experimentally known core (even-even) spectra are insufficient for calculation of the available spectra of the neighboring odd nuclei. In these cases the experimental core spectra have been extrapolated to get the energies of the higher spin core states. The satisfactory theoretical reproduction of the odd-A spectra justifies this core simulation. The branching ratios are also calculated and compared with the experimental ones, wherever available. In a few cases, ambiguity in level ordering has been resolved and spin-parities have been assigned to the levels. Thus such calculations can be used for proper identification of levels and assignment of spin-parities for those nuclei whose experimental investigations are very difficult and involved.

II. MODEL

A. Formalism

The model is based on the assumption that the nucleus under consideration is axially symmetric. In this model, the motion of an unpaired quasiparticle in a deformed Nilsson orbit is coupled to the rotational motion of the core through the Coriolis interaction. We have used a version [9] of the PRM in which the experimental core level energies can be fed directly as inputs.

The Hamiltonian of the odd-A system can be written as

$$H = H^0_{qp} + c\mathbf{R}\cdot\mathbf{j} + E_c(R). \tag{1}$$

The first term is the Hamiltonian of a single quasiparticle and is given by

$$H^0_{qp} = \sum_K E_K a^\dagger_K a_K, \tag{2}$$

with

$$E_K = \sqrt{(\epsilon_K - \lambda)^2 + \Delta^2}, \tag{3}$$

where ϵ_K is the energy of a single particle moving in an axially symmetric Nilsson potential. The pairing gap and the Fermi level are represented by Δ and λ, respectively.

The last term, $E_c(R)$, represents the collective part of the Hamiltonian, whereas the middle term describes the rotational dependence of the interaction between the core and the quasiparticle. The coefficient c is defined [9] in terms of the core moment of inertia corresponding to the lowest 2^+ state in the rotational band and another parameter α. For a constant moment of inertia, α is identical to the usual Coriolis attenuation factor. Moreover, it can be shown that introduction of the $c\mathbf{R}\cdot\mathbf{j}$ term in the Hamiltonian effectively reduces the recoil energy if there is attenuation of the Coriolis matrix elements. In the limit of very small attenuation ($\alpha \simeq 1$), this interaction term loses its significance. It can be shown [9] that, in the present formalism, the Coriolis attenuation factor will, in general, be a function of the angular momentum (I) of the excited state.

The basis states are usually taken in the form

$$|IMK\rangle = [(2I+1)/8\pi^2]^{1/2} \times \left[\mathcal{D}^I_{MK}\chi_K + (-)^{I-1/2}\mathcal{D}^I_{M,-K}\chi_{-K}\right]/\sqrt{2}. \tag{4}$$

Here χ_K represent the Nilsson single-particle states that can be expanded into eigenstates of j^2,

$$\chi_K = \sum_j C_{jK} \mid jK\rangle. \tag{5}$$

However, we have to transform the basis into a representation with sharp R and j to calculate the R-dependent terms in the Hamiltonian [9].

The total Hamiltonian [Eq. (1)] is diagonalized, giving the energy eigenvalues and the wave functions of the final states $|IM\rangle$ in terms of the Coriolis mixing amplitudes f_{IK} and the basis states $|IMK\rangle$.

$$|IM\rangle = \sum_K f_{IK}|IMK\rangle. \tag{6}$$

To calculate a state with total angular momentum I, where the single particle angular momentum involved is j (say), the experimental core energies required will be given by the following range of R values,

$$\begin{aligned} R_{\max} &= I + j \\ R_{\min} &= I - j. \end{aligned} \tag{7}$$

B. Parameter choice

There are several parameters involved in the PRM calculations (Table I). To reduce arbitrariness in calculations, we have tried to fix as many of them as possible either from experimental observables or from previous calculations. The single-particle Nilsson parameters μ and κ in each individual nucleus have been deduced from the prescription of Nilsson *et al.* [11]. We have also checked our calculations with the new μ and κ values deduced specifically for the ^{132}Sn region [12]. The calculations for ^{137}I and ^{137}Te show better results with the μ and κ values from Ref. [11], but for ^{139}Xe, the new μ and κ values from Ref. [12] give better results. We have kept our choices of μ and κ fixed to these suggestions to reduce the number of adjustable parameters. It is seen that the intraband spacings are almost independent of this choice. The ground state deformation parameter $\delta(=0.95\beta)$ is obtained from β values extracted from the experimental B(E2) [5] in the neighboring even-even nuclei. The pairing gap parameter (Δ) is calculated from the odd-even mass difference (Δ_{o-e}) [13]. In most of the nuclei, Fermi levels λ are adjusted to reproduce the experimental ground state spins and parities. Only in a few exceptional cases has λ been modified to have better agreement with experimental results within the band. The only totally free parameter, the ad-hoc attenuation coefficient α, is varied from 1.0 to 0.7 to get theoretical energy values close to experimental results.

The choice of the core needs a special mention unlike in the usual cases of such calculations [9]. We have fed in the experimental excitation energies of the neighboring even-even core as input parameters, wherever available. But in some of the cases the experimental spectrum of the core [see Eq. (7)] was insufficient (only a few states of the ground band of the core were known) to reproduce the experimental spectrum of the odd-A nucleus. For those cases we have fitted the energies of the core states E_R to be a quadratic function of R, the functional form being $E_R = A + BR + CR^2$. But the core

TABLE I. Parameters used for PRM calculations in different nuclei. The symbols have their usual meanings, as discussed in Sec. II. Energies are in MeV.

Isotope	μ	κ	δ	Δ	λ	State	α	Core
$^{137}_{52}Te_{85}$								
Set I	0.455	0.064	0.065	0.56	51.0	1/2[541] (92% $2f_{7/2}$)	0.896	^{136}Te (expt.+fitted($16^+ - 22^+$))
Set II	"	"	"	"	52.5	5/2[512] (69% $1h_{9/2}$)	0.90	"
$^{139}_{52}Te_{87}$	0.455	0.064	0.1045	0.75	49.8	1/2[541] (79% $2f_{7/2}$)	0.66	^{138}Te (expt.+fitted($12^+ - 18^+$))
$^{137}_{53}I_{84}$	0.582	0.066	0.065	0.77	44.4	3/2[422] (95% $1g_{7/2}$)	0.95	^{136}Te (expt.+fitted($16^+ - 22^+$))
$^{139}_{53}I_{86}$	0.583	0.066	0.09	0.61	44.2	1/2[420] (88% $2d_{5/2}$)	0.97	^{138}Te (expt.+fitted($12^+ - 18^+$))
$^{139}_{55}Cs_{84}$	0.583	0.066	0.029	0.991	44.359	5/2[413] (99% $1g_{7/2}$)	0.975	^{138}Xe (expt.+fitted($16^+ - 24^+$))
$^{139}_{54}Xe_{85}$								
Negative parity								
Set I	0.09	0.035	0.03	0.91	51.519	1/2[530] (75% $3p_{3/2}$)	0.98	^{138}Xe (expt.+fitted($16^+ - 24^+$))
Set II	0.452	0.0637	0.12	0.91	50.55	1/2[541] (72% $2f_{7/2}$)	0.835	-do-
Positive parity	0.452	0.0637	0.12	0.91	52.097	5/2[642] (98% $1i_{13/2}$)	0.977	-do-
$^{141}_{54}Xe_{87}$								
Negative parity	0.45	0.0637	0.108	0.92	51.5	5/2[523] (55% $1h_{9/2}$)	0.95	^{140}Xe (expt.)
Positive parity	0.45	0.0637	0.108	0.92	57.67	1/2[651] (85% $2g_{9/2}$)	1.0	-do-
$^{141}_{56}Ba_{85}$								
Negative parity	0.45	0.0637	0.12	0.91	49.7	1/2[541] (72% $2f_{7/2}$)	0.88	^{140}Ba (expt.+fitted($12^+ - 30^+$))
Positive parity	0.45	0.0637	0.12	0.91	49.7	1/2[660] (96% $1i_{13/2}$)	0.975	-do-

nuclei (Table I) are mostly vibrational in nature with R_4 values ranging from 1.7 to 2.2. This is also reflected in the fitted values of C for the cores. These values (in MeV) lie between 0.001 and 0.010, much smaller than the values of B lying between 0.180 and 0.251. These values thus indicate a linear rather than a parabolic dependence of $E(R)$ and a vibrational, not a rotational, character of these nuclei.

We have calculated the electromagnetic properties in both odd neutron and proton nuclei. Corrections for conversion coefficients have been neglected. As only E2 and M1 transitions are considered and the energies of the γ rays are also more than 180 keV, the contribution from conversion is negligible (maximum $\simeq 2\%$). Transition probabilities for odd-proton nuclei are calculated with $g_l^p = 1, (g_s)_{\rm eff}^p = 0.6 g_s^p = 3.35$, $g_R = Z/A$, and $(e_p)_{\rm eff} = 1.5e$. For odd-neutron nuclei, calculations are done with $g_l^n = 0$, $(g_s)_{\rm eff}^n = 0.6 g_s^n = -2.30$, $g_R = Z/A$, and $(e_n)_{\rm eff} = 0.5e$. Experimental γ energies have been used in the calculation of transition probabilities.

III. RESULTS AND DISCUSSIONS

A. The shell model wave functions of ^{137}Te and ^{137}I and justification of PRM calculations

For ^{137}I, the shell model (SM) wave functions show substantial configuration mixing. For the $7/2^+$ ground state, configurations belong to 15 different nucleon partitions, each contributing more than 1% mix, with the most dominant contribution being 37% from a single partition. The same feature is observed for other spins up to $33/2^+$. PRM also reproduces the energy eigenvalues of these levels reasonably well (Fig. 1). Moreover, the order of the $9/2^+$ and $11/2^+$ levels has been reproduced correctly in PRM unlike in SM.

Similar features can be found (Fig. 2) for ^{137}Te up to $27/2^-$. For higher spins (as also for $25/2^-$) shell model

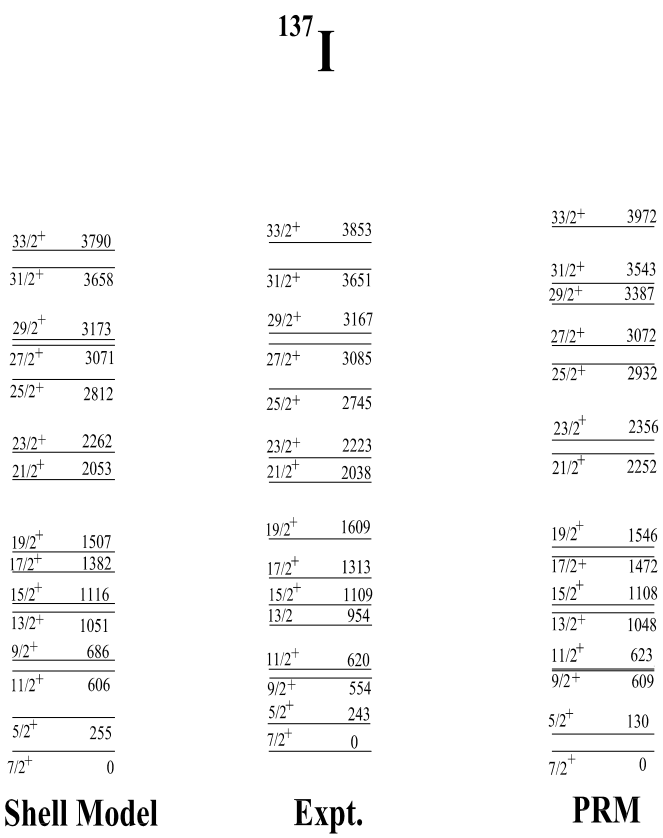

FIG. 1. The experimental spectra of the positive parity states in ^{137}I are compared with shell model (SM) and PRM results.

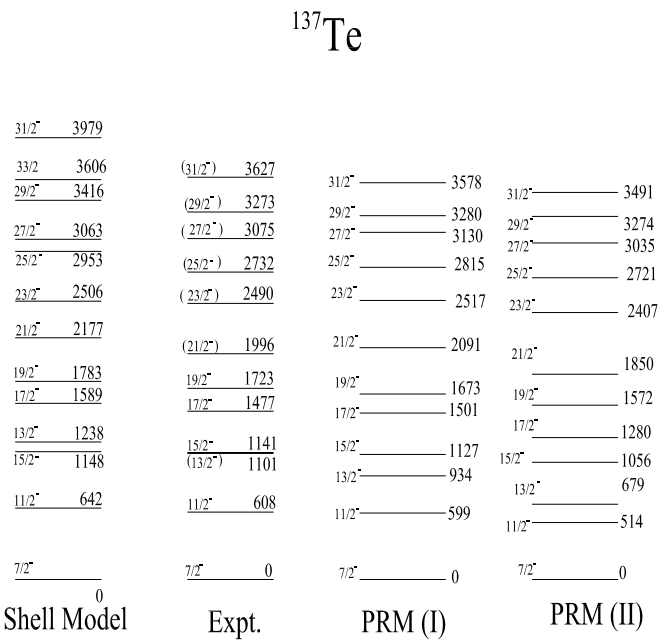

FIG. 2. The experimental spectra of the negative parity states in ^{137}Te are compared with shell model (SM) and PRM results.

results show poorer agreement and wave fuctions also show a new feature, an increase in configuration mixing having only maximum 26% contribution from a single partition. Both PRM calculations show better agreement for most of the spin values except for the $11/2^-$, $13/2^-$, and $21/2^-$ levels in PRM(II). PRM(II) (Table I) shows the results from a calculation with a change in the Fermi level. This set shows a better agreement with the branching ratio data (Table II). As pointed out in [2], the spectra of ^{137}Te and ^{137}I show a kind of regularity, a clear indication of signature splitting. This regularity, composition of the SM wave functions of the levels, and the agreement of the PRM calculations with the experimental results are indicative of mild deformation and consequent onset of collectivity in both the nuclei. Lack of adequate experimental information on the lifetimes/transition probabilities fails to provide direct evidence for collectivity. Recent experimental results for the more neutron-rich Te, I, Xe, Cs, and Ba isotopes show increasing collectivity with increasing neutron number and the PRM seems to be an appropriate simple phenomenological model for studying the structure of these nuclei. It is important to point out here that though there are not yet any experimental results for more n-rich ^{137}Sn ($Z = 50, N = 82 + 5$),^{138}Sn ($Z = 50, N = 82 + 6$), and ^{137}Sb ($Z = 51, N = 82 + 4$) nuclei, the shell model calculations show [14] no signature of collectivity in these nuclei. The structures of the low-lying yrast and near yrast levels in these nuclei are dominated mostly by a single partition. In contrast, the spectra of the $A = 137$, Te ($Z = 50 + 2, N = 82 + 3$) and I ($Z = 50 + 3, N = 82 + 2$) nuclei, with more than one neutron and proton in the valence space, show mild collectivity. Considerations for the spectra of other heavier Te, Xe, Ba isotopes also indicate that the appearance of collectivity in the yrast levels occurs for nuclei with more than one neutron and proton in the valence space. But it is still not clear how the onset and evolution of collectivity in these n-rich nuclei exactly depend on the number of valence neutrons and protons. This seems to be an important issue for this mass region and warrants further investigation.

TABLE II. Comparison of experimental and calculated branching ratios. E_γ indicates the γ-ray energy connecting the initial and final states. All energies are quoted in MeV. Branching ratios are quoted as percentages (%).

J_i (Energy)	J_f (Energy)	E_γ	Branching ratio	
			Expt.	Theo
	⟨^{137}Te (negative parity): Set I (Set II)⟩			
17/2(1.477)	15/2(1.141)	0.336	More	39 (72)
	13/2(1.101)	0.377	Less	61 (28)
19/2(1.723)	17/2(1.477)	0.246	More	20 (3)
	15/2(1.141)	0.582	Less	80 (97)
21/2(1.996)	19/2(1.723)	0.273	More	0.5 (30)
	17/2(1.477)	0.519	Less	99.5 (70)
25/2(2.732)	23/2(2.490)	0.242	Less	46 (8)
	21/2(1.996)	0.736	More	54 (92)
	⟨^{137}I (positive parity)⟩			
13/2(0.954)	11/2(0.620)	0.334	21	20
	9/2(0.554)	0.400	79	80
19/2(1.609)	17/2(1.313)	0.296	88	70
	15/2(1.109)	0.500	12	30
21/2(2.038)	19/2(1.609)	0.429	4	1
	17/2(1.313)	0.725	96	99
23/2(2.223)	21/2(2.038)	0.185	34	18
	19/2(1.609)	0.614	66	82
25/2(2.743)	23/2(2.223)	0.520	23	2
	21/2(2.038)	0.705	77	98
27/2(3.085)	25/2(2.743)	0.342	8	20
	23/2(2.223)	0.862	92	80
	⟨^{139}I (positive parity)⟩			
13/2(0.816)	11/2(0.435)	0.381	10	13
	9/2(0.419)	0.397	90	87
17/2(1.280)	15/2(0.929)	0.351	18	4
	13/2(0.816)	0.464	82	96
	⟨ ^{139}Cs (positive parity)⟩			
13/2(1.070)	11/2(0.602)	0.468	Less	31
	9/2(0.595)	0.475	More	69
	⟨^{139}Xe (negative parity): Set I (Set II)⟩			
9/2(0.560)	7/2(0.023)	0.537	60	0.5(7)
	5/2(0.032)	0.528	40	99.5(93)
19/2(1.810)	17/2(1.577)	0.233	8	2 (2.4)
	15/2(1.179)	0.631	92	98 (97.6)
21/2(2.159)	19/2(1.810)	0.349	12	0.2 (0.1)
	17/2(1.577)	0.582	88	99.8 (99.9)
23/2(2.500)	21/2(2.159)	0.341	16	47 (0.2)
	19/2(1.810)	0.690	84	53 (99.8)

B. Comparison of PRM results with energy and branching ratio data

The calculated excitation energies are compared with the experimental values for the nuclei ^{137}I,^{137}Te, ^{139}Te, ^{139}I,^{139}Xe, ^{139}Cs, ^{141}Ba, and ^{141}Xe in Figs. (1–8). The excitation energies

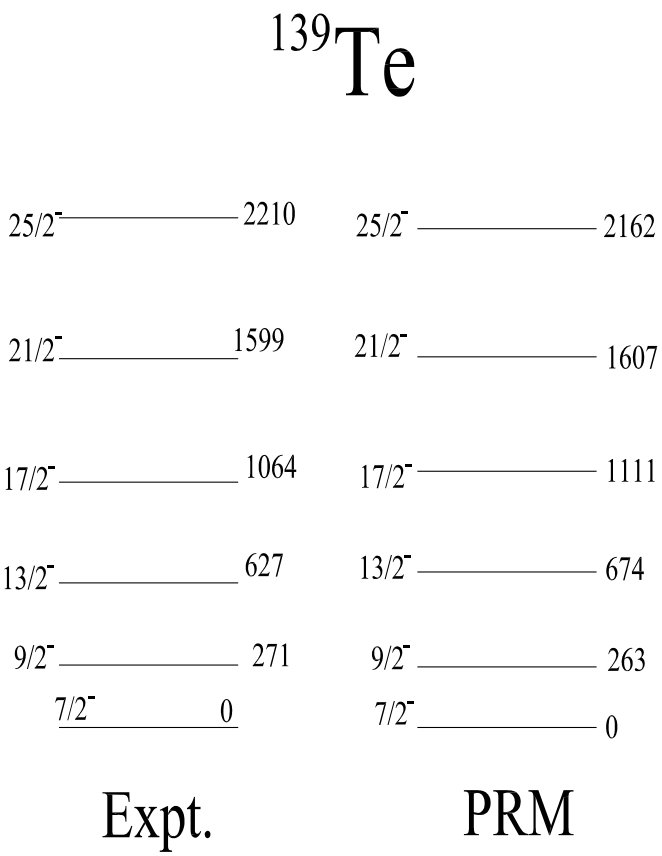

FIG. 3. The experimental spectra of the negative parity states in ^{139}Te are compared with PRM results.

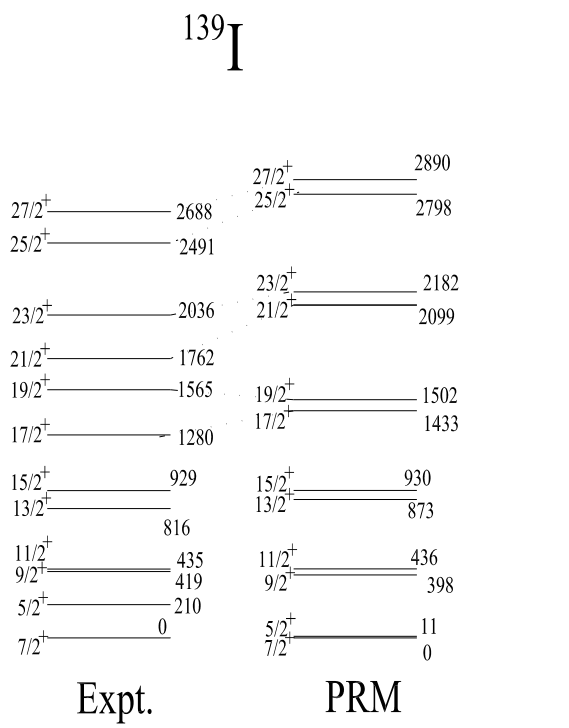

FIG. 4. The experimental spectra of the positive parity states in ^{139}I are compared with PRM results.

of the levels are given in keV with respect to the energies of the corresponding band heads. For ^{137}Te and ^{137}I, shell model results [2] are displayed in Figs. 1 and 2 along with the PRM results. There is no experimental information about the lifetimes of the states. In most of the cases quantitative estimation for intensities of the transitions are not reported. The relative intensities are indicated by the thicknesses of the arrows in the figure of the level scheme. We have determined experimental branching ratios for the cases where intensity values are mentioned. For the rest, the relative thicknesses of the arrows are compared with the theoretical numbers to test the wave functions. The overall agreement of theoretical results with the data is reasonable. The nature of agreement and structural details of the states are discussed separately for each nucleus.

(i) ^{137}Te [15]. The relative intensities are not available in the literature. The energy values are reproduced quite well using Set I parameters (Fig. 2). But these wave functions do not reproduce well the branching ratio results (Table II). The wave function decomposition shows structural differences between signature partners at lower spins that gradually diminish as one goes up in spin. The signature $-1/2$ states arise primarily from the $2f_{7/2}$ contribution, whereas the signature $+1/2$ partners have $1h_{9/2}$ as the dominant contributor. For improvement in the reproduction of branching ratios, the Fermi level has been shifted (Table I, Set II) near $5/2^-[512]$, originating primarily from the $1h_{9/2}$ orbital. Although the calculated branching ratios show some improvement, the agreement in energies deteriorates. The structural differences between the partners are no longer clean like those in Set I.

(ii) ^{139}Te [16]. This is the most neutron-rich odd Te isotope, for which the excited states are known experimentally. The heavy Te isotopes are expected to show a shape transition from spherical to prolate between ^{136}Te and ^{140}Te. It has been indicated in Ref. [16] that the shape transition takes place at ^{139}Te with $N = 87$. This is also supported by our result. The theoretical results show extremely good agreement with the experimental data (Fig. 3). No transition probability data are available for this nucleus. The results show that the yrast states, namely, $7/2^-$, $9/2^-$, $13/2^-$, $17/2^-$, $21/2^-$, and $25/2^-$, observed experimentally belong to the Nilsson $1/2^-[541]$ band, originating primarily from the $2f_{7/2}$ orbital. The unobserved yrast states, namely, $11/2^-$, $15/2^-$, $19/2^-$, and $23/2^-$, originate from the $1/2^-[530]$ band arising from the $1h_{9/2}$ orbital. Assigning the $1/2^-[541]$ configuration to the ground state band in ^{139}Te, which has five neutrons outside ^{132}Sn, needs some discussion. As some of the $-1/2$ signature members of the band are still unobserved, the choice of Fermi level has some arbitrariness. For example, a Fermi level at 53.2 MeV (on the $7/\,2^-[503]$ orbital originating from $2f_{7/2}$) gives almost similar results for the observed levels. But for other choices of λ near orbitals originating from $1h_{9/2}$, the agreement is grossly disturbed. More experimental data on the $-1/2$ signature members are therefore needed.

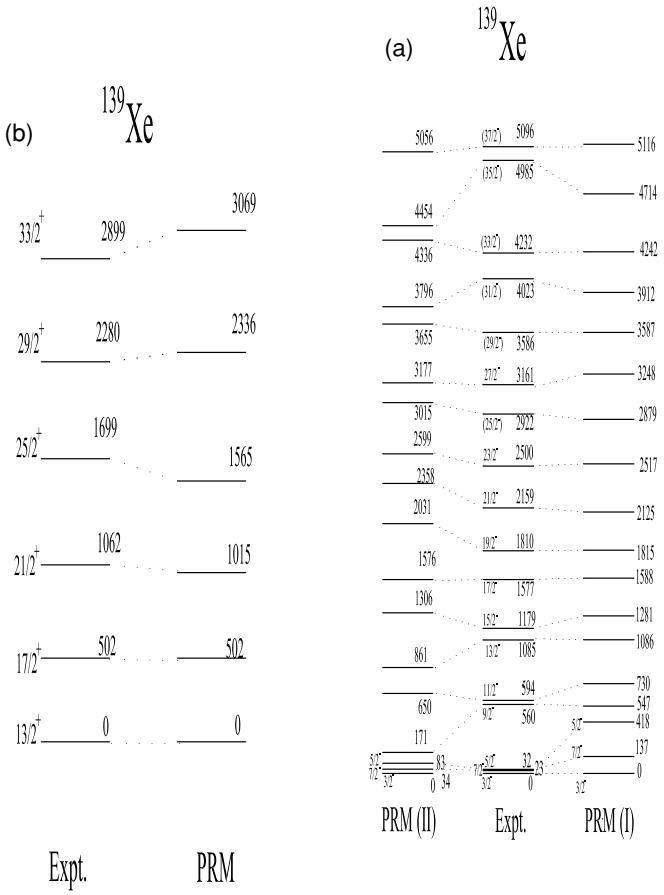

FIG. 5. The experimental spectra of ^{139}Xe are compared with PRM results. Results are shown for the (a) negative and (b) positive parity states.

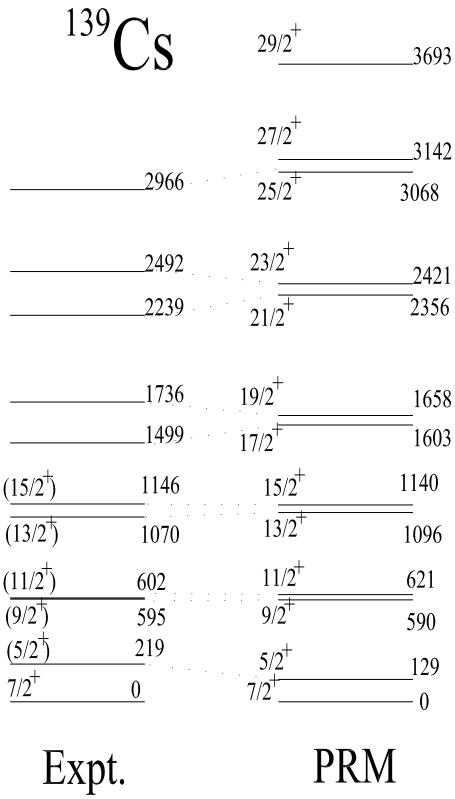

FIG. 6. The experimental spectra of the positive parity states in ^{139}Cs are compared with PRM results.

For heavier isotopes of Te, predictions from this model can provide guidance to the experimentalists.

(iii) ^{137}I [17]. For this nucleus, both energies and branching ratios are reproduced using the same parameter set (Fig. 1). The signature partner states do not have much structural difference. Apart from the $5/2^+$ state, they arise predominantly from the Nilsson orbitals originating from $1g_{7/2}$.

(iv) ^{139}I [6]. For this odd-proton nucleus, a situation similar to that in ^{137}I is seen. Both energies and branching ratios are reproduced using the same parameter set (Fig. 4). The signature partner states have structural differences. The signature $-1/2$ arises primarily from $1g_{7/2}$, whereas the signature $+1/2$ partners have $2d_{5/2}$ as the dominant contributor.

(v) ^{139}Xe [7,8]. In the negative parity band, both energies and branching ratios are reproduced using the same parameter set [Fig. 5(a)]. Regarding the structure of the states, a situation similar to that in ^{137}Te (Set I) is seen. The signature partner states have clear structural differences. The signature $-1/2$ arises primarily from the $2f_{7/2}$ contribution, whereas the signature $+1/2$ partners have $1h_{9/2}$ as the dominant contributor. We also show a result with another set of parameters (Set II, Table I). The branching ratios are similar with both sets but the signature splitting has been reproduced better with Set I. The positive parity band and its correlation with the negative parity one are discussed in the next subsection.

(vi) ^{139}Cs [18,19]. For odd-proton ^{139}Cs, the agreement between the theory and the experiment [18] is quite reasonable (Fig. 6). The signature splitting is well reproduced up to $15/2^+$. But for higher spins it is more pronounced in the theoretical spectra compared to that in the experimental spectra. The bands originate primarily from the $1g_{7/2}$ orbital. Levels with unassigned spins above 1146 keV were assigned spin values by comparison with the theoretical level scheme. The results clearly distinguish between the two proposed level schemes [18,19] and act as a strong justification in favor of the scheme proposed in Ref. [18].

C. Octupole correlation and ^{141}Ba$_{85}$, ^{139}Xe$_{85}$, and ^{141}Xe$_{87}$

Luo *et al.* and Zhu *et al.* [7] proposed strong octupole correlations in these nuclei. But later Urban *et al.* [8] contradicted this proposition. They corrected some of the previous spin assignments. The excitations in $N = 85$ isotones were interpreted by them as quadrupole and octupole vibrations coupled to the valence neutron orbitals. Although the study of strong octupole correlation or its coupling with quadrupole vibrations is beyond the scope of the present model, our results in the other $N = 85$ isotones, ^{137}Te, motivated us to

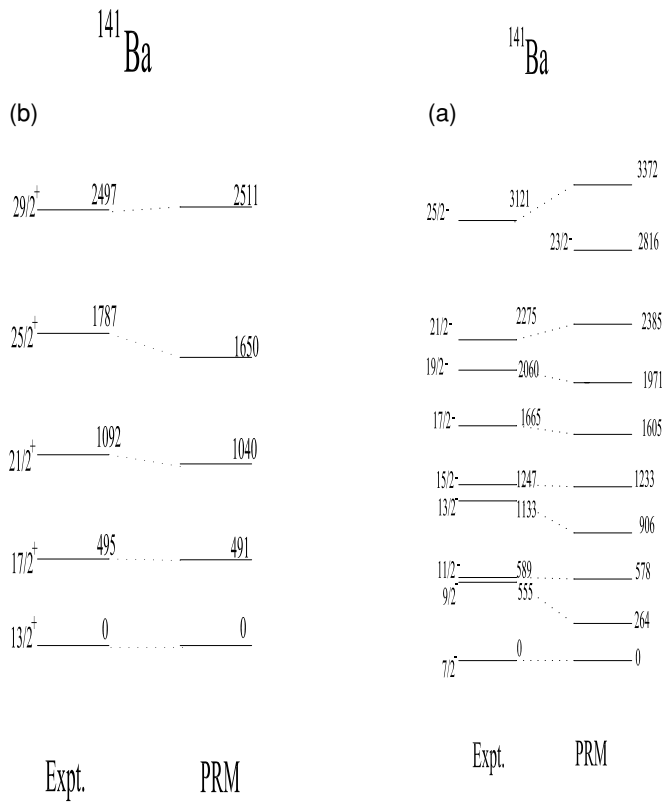

FIG. 7. The experimental spectra of ^{141}Ba are compared with PRM results. Results are shown for the (a) negative and (b) positive parity states.

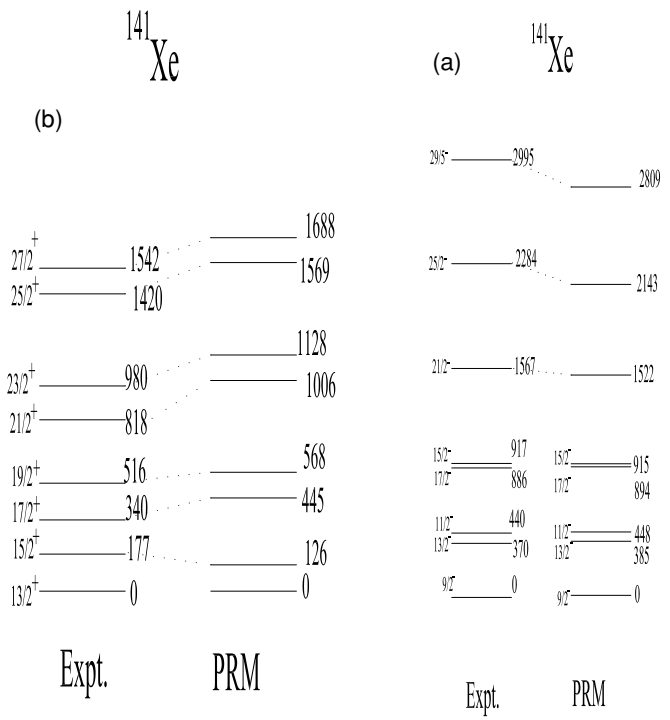

FIG. 8. The experimental spectra of ^{141}Xe are compared with PRM results. Results are shown for the (a) negative and (b) positive parity states.

apply this model to Ba and Xe isotopes also. In nuclei with strong octupole correlations, the positions and identities of the Nilsson orbitals are changed significantly, but in the limit of weak correlation they may be used in the first approximation. Based on this assumption, the present model was applied to study these bands.

The results show some interesting features. The negative parity bands (arising predominantly from $2f_{7/2}$ and $1h_{9/2}$ orbitals) in both $^{141}Ba_{85}$ [Figs. 7(a) and 7(b)] and $^{139}Xe_{85}$ [Figs. 5(a) and 5(b)] show reasonable agreement, apart from some disagreement at the low energies. The relative band head energy differences between the positive and negative parity bands are not reproduced well. This is because of our choice of Nilsson parameters. The proper choice of these parameters reproduces the band heads exactly. For ^{141}Ba, keeping all other parameters the same as in Table I, if the value of μ for $N = 6$ shell is changed to 0.3985 the theoretical band head energy of the observed positive parity band comes at 1285 keV, exactly the same as that observed experimentally. The agreement of the positive parity band also remains similar to that in Fig. 7. Similarly for ^{139}Xe with μ=0.32 and Fermi level at 50.55 MeV (same as that for the negative parity band in Table I, Set II), the theoretical band head energy comes at 1.534 MeV (experimental value is 1.512 MeV). Moreover it has also been observed [20] that some adjustment in the single particle energies of one or two levels are necessary to reproduce the lower energy part of the spectrum of a particular isotope. But intraband spacings are usually almost insensitive to this choice. So we have tried not to play with these parameters. For the positive parity bands (the so-called positive parity partners in the octupole band) in both these nuclei there is good agreement with the theory. They can be interpreted as decoupled bands based on Nilsson orbitals originating from $1i_{13/2}$. So the agreement in the parity partner bands may indicate that octupole correlation does not exist in these nuclei. Even if it exists, it has only perturbative effects. So the two bands retain their identity as far as their level spectra are concerned. However, comparison of energy eigenvalues only is not enough to resolve that these bands do not originate because of octupole correlation. Precise information on the lifetime may be important to resolve this ambiguity. In ^{141}Xe [21] [Figs. 8(a) and 8(b)], the negative parity band arising predominantly from $1h_{9/2}$ shows better agreement with theory. In this nucleus, the positive parity band is a $\Delta I = 1$ band, unlike those in $^{141}Ba_{85}$ [Fig. 7(b)] and $^{139}Xe_{85}$ [Fig. 5(b)], where they are $\Delta I = 2$ bands. It can only be reproduced theoretically for Fermi level positions near $1/2^+[651]$ originating from $2g_{9/2}$ ($\simeq$85%). The calculation also involves all the orbitals from $N = 6$ instead of only those from $1i_{13/2}$.

IV. CONCLUSION

The present calculations show that the simple version of the PRM with the experimental core energies as the input is quite capable of explaining the level sequences and their origins in the odd-A neutron-rich nuclei in the ^{132}Sn region. They also show that the simulated energies for the higher spin states of the core can reproduce the spectroscopic properties of the

neighboring odd-*A* nuclei quite satisfactorily. It seems that the octupole correlation expected in some of these nuclei has only a perturbative effect. More data on transition probability are needed to comment conclusively on this effect. The present work indicates that the appearance of collectivity even in the yrast levels depends delicately on the valence neutron and proton numbers. This seems to be an important issue for this mass region and warrants further experimental and theoretical investigations.

ACKNOWLEDGMENT

The authors thank Professor S. Sen and Professor S. Bhattacharya for the computer code.

[1] Sukhendusekhar Sarkar and M. Saha Sarkar, Phys. Rev. C **64**, 014312 (2001), and references therein.
[2] Sukhendusekhar Sarkar and M. Saha Sarkar, Eur. Phys. J. A **21**, 61 (2004), and references therein; Sukhendusekhar Sarkar, Proc. DAE-BRNS Symp. Nucl. Phys. (India) **45A**, 72 (2002).
[3] L. Coraggio, A. Covello, A. Gargano, and N. Itaco, Phys. Rev. C **73**, 031302(R) (2006), and references therein; D. J. Dean, T. Engeland, M. Hjorth-Jensen, M. P. Kartamyshev, E. Osnes, Prog. Part. Nucl. Phys. **53**, 419 (2004).
[4] Data extracted using the NNDC On-line Data Service from ENSDF and XUNDL databases.
[5] S. Raman, C. W. Nestor Jr., and P. Tikkanen, At. Data Nucl. Data Tables **78**, 1 (2001).
[6] W. Urban *et al*., Phys. Rev. C **65**, 024307 (2002), and references therein.
[7] Y. X. Luo *et al*., Phys. Rev. C **66**, 014305 (2002); S. J. Zhu *et al*., J. Phys. G **23**, L77 (1997).
[8] W. Urban *et al*., Phys. Rev. C **66**, 044302 (2002).
[9] E. M. Müller and U. Mosel, J. Phys. G **10**, 1523 (1984); M. Saha, A. Goswami, S. Bhattacharya, and S. Sen, Phys. Rev. C **42**, 1386 (1990).
[10] M. Saha Sarkar, Phys. Rev. C **60**, 064309 (1999).
[11] S. G. Nilsson, C. F. Tsang, A. Sobiczewski, Z. Szymanski, S. Wycech, C. Gustafson, I. L. Lamm, P. Moller, and B. Nilsson, Nucl. Phys. **A131**, 1 (1969).
[12] Jing-ye Zhang, Yang Sun, Mike Guidry, L. L. Riedinger, and G. A. Lalazissis, Phys. Rev. C **58**, R2663 (1998).
[13] G. Audi and A. H. Wapstra, Nucl. Phys. **A565**, 1 (1993).
[14] S. Sarkar and M. Saha Sarkar, nucl-th/0503067, 28 Mar 2005; JINA-Virt. J. Nuc. Astrophys. Vol. 3, Issue 13 (2005); S. Sarkar and M. Saha Sarkar, Proc. DAE-BRNS Symp. Nucl. Phys. (India) **47B**, 58 (2004).
[15] W. Urban *et al*., Phys. Rev. C **61**, 041301(R) (2000).
[16] W. Urban *et al*., Phys. Rev. C **62**, 044315 (2000).
[17] A. Korgul *et al*., Eur. Phys. J. A **12**, 129 (2001).
[18] A. Nowak *et al*., Eur. Phys. J. A **6**, 1 (1999).
[19] J. K. Hwang *et al*., Phys. Rev. C **57**, 2250 (1998).
[20] S. Bhattacharya, S. Sen, and R. K. Guchhait, Phys. Rev. C **32**, 1026 (1985).
[21] W. Urban *et al*., Eur. Phys. J. A **8**, 1 (2000).